Likelihood Ratio Test-Based Chart for Monitoring the Process Variability

Jiujun Zhang [a], Chuan He [b], Zhonghua Li [c], Zhaojun Wang [c,*]

[a] *Department of Mathematics, Liaoning University, Shenyang 110036, P.R.China*

[b] *Department of Mathematics, Northeastern University, Shenyang 118019, P.R.China*

[c] *LPMC and Institute of Statistics, Nankai University, Tianjin 300071, P.R.China*

Abstract

This paper proposes a new chart with the generalized likelihood ratio (GLR) test statistics for monitoring the process variance of a normally distributed process. The new chart can be easily designed and constructed and the computation results show that it provides quite a satisfactory performance, including the detection of the decrease in the variance and the individual observation at the sampling point which are very important in many practical applications. Average run length comparisons between other procedures and the new chart are presented. The optimal parameters that can be used as a design aid in selecting specific parameter values based on the average run length (ARL) are described. The application of our proposed method is illustrated by a real data example from chemical process control.

Key words: Likelihood Ratio Test; Exponentially Weighted Moving Average; Average Run Length; Statistical Process Control
1991 MSC: 62P30

1 Introduction

Control charts are effective statistical process control (SPC) tools that have been widely used in industries for monitoring the quality of processes. Among them, monitoring the increase in the process variance is one of the main fields

* Corresponding author.
Email addresses: zjjly790816@163.com (Jiujun Zhang), hexiaodong9@163.com (Chuan He), zli@nankai.edu.cn (Zhonghua Li), zjwang@nankai.edu.cn Tel: 86-22-23498233 Fax: 86-22-23506423 (Zhaojun Wang).

in SPC that leads the output of the process to be more scattered. It is well known that if the variance increases then an increased number of units will be defective. Collani and Sheil (1989) indicated that some manufacturing circumstances may lead to an increase in process variability without influencing the level of the process mean. On the other hand, when the process variance decreases then more units will be closer to the target value. The decrease in the process dispersion that leads the output of the process to be more concentrated should also be recognized (Nelson, 1990) since it may indicate ways to improve the process. These charts are also important when interpreting the results of a mean chart since it assumes that the process standard deviation remains constant. Thus, identifying process dispersion changes is a crucial ingredient of SPC to ultimately improve product quality and process productivity, which is the focus of this paper.

Shewhart R and S charts are basic tools to monitor the shifts in process dispersion, but both charts are effective in detecting large shifts and less effective for small shifts because they are based only on the information of the current sample. Consequently, Page (1963) proposed a one-sided CUSUM chart and a Shewhart chart with warning lines based on R to detect the increase in process standard deviation. Alt (1984) discussed Shewhart sample variance S^2 chart and S chart. Tuprah and Ncube (1987) made a comparison of dispersion control charts. Ng and Case (1989) proposed an exponentially weighted moving average (EWMA) dispersion chart based on the subgroup range. Crowder and Hamilton (1992) developed a onesided EWMA based on the natural log of the subgroup variance. Chang and Gan (1994) investigated the effect of reflecting boundaries and proposed a one-sided EWMA chart based on ln S^2 to detect the decrease in process standard deviation.

In recent several years, Huang and Chen (2005) proposed a synthetic control chart for monitoring process dispersion with sample standard deviation. Castagliola (2005) proposed a chart based on a three-parameters logarithmic transformation combined with an EWMA approach to monitor the sample variance. Knoth (2006) evaluated the performance of CUSUM charts based on S^2 for normal processes. Castagliola et al. (2007) introduced a variable sampling interval S^2-EWMA chart for monitoring process variance. Shu and Jiang (2008) proposed a new EWMA dispersion chart by truncating negative normalized observations to zero in the traditional EWMA statistic. Riaz (2008) proposed a Q chart based on the interquartile range for monitoring changes in process dispersion. Riaz and Saghir (2009) proposed a mean deviation based approach to monitor process variability. Castagliola and Maravelakis (2009) developed an EWMA chart for monitoring the process standard deviation when parameters are estimated. Castagliola et al. (2009) proposed a new CUSUM S^2 chart for monitoring the process variance. Montgomery (2009) suggested several charts to monitor the process dispersion. Human et al. (2010) studied the Shewhart-type S^2, S and R charts when the mean and

variance of the process are estimated from the preliminary data. Huwang et al. (2010) proposed EWMA control charts for monitoring process dispersion. Zhang et al. (2011) developed an adaptive Shiryaev-Roberts procedure with EWMA estimation for monitoring the dispersion over a range of variance shifts.

Apart from the references mentioned above, Abbasi et al. (2012) developed two sensitizing rules in CUSUM dispersion chart to enhance the ability to detect smaller changes in process variability. Abbas et al. (2013a) proposed a memory-type control chart based on logarithmic transformation of the sample variance. Abbas et al. (2013b) proposed another two new memory-type control chart for monitoring the process variance. Barbosa et al. (2013) presented simpler alternative formulae and procedures of implementation to deal with the relative range statistic used in the range control chart for process dispersion monitoring. Abbasi and Miller (2013) proposed an alternative EWMA dispersion chart based on the mean absolute deviation from the median. Riar (2013) investigated a set of interquartile range charts to monitor process dispersion. Nazir et al. (2013a,b) proposed robust CUSUM and Shewhart control charts for process dispersion, respectively. Riaz et al. (2014) developed a set Shewhart-type variability control chart based on the utilization of auxiliary information for efficient Phase II process monitoring. Schoonhoven and Does (2012) proposed a standard deviation control chart that is robust against both diffuse disturbances and localized disturbances. Schoonhoven et al. (2011) concerned the design and analysis of standard deviation control chart with estimated parameters. Ahmad et al. (2013) proposed a control chart for monitoring process variability under double sampling scheme. Ahmad et al. (2014) considered efficient use of auxiliary information for control charting.

All of the foregoing charts are shown to have satisfactory performance, however, most of the charts are based on the sample variance S^2, that is to say, the sample size must be larger than one. In such case, these charts may not be appropriately used in the case that only an individual observation is available at one sampling point. In addition, when the aim is to detect the increase and decrease in the process variance simultaneously, a satisfied method is to use a single chart. When a single chart is used, the design and operation of the monitoring scheme can be greatly simplified compared with the combination-type chart. Unfortunately, most of the existing charts cannot be used for this purpose in this case. To this end, in this paper, we propose a dispersion chart based on GLR test statistics integrating the EWMA procedure. The proposed chart can be easily designed and constructed, can effectively detect the increase and decrease in variability and is able to handle the case that the sample size is one.

The rest of this paper is organized as follows. In the next section, some of the existing competing charts are briefly reviewed. In Section 3, our new chart is

introduced. After that, the optimal design of the new charts is discussed in Section 4 and its run-length distribution is presented in Section 5. We compare the performance of the proposed chart with the three existing charts in terms of ARL in Section 6. The application of our proposed method is illustrated by a real data example from chemical process control in Section 7. Several remarks conclude the article in the last Section.

2 The existing charts

In this section, we briefly introduce three competing dispersion charts that are widely used in literature to handle dispersion issue based on the ARL performance. They are: the EWMA chart based on $\ln S^2$ proposed by Crowder and Hamilton (1992) (denoted as CH chart), the EWMA chart suggested by Shu and Jiang (2008) (denoted as SJ chart) and the change point CUSUM chart proposed by Acosta et al. (1999) (denoted as CPC chart).

2.1 The EWMA CH chart:

Let $Y_t = \ln S_t^2$, where $S_t^2 = \frac{1}{n}\sum_{i=1}^{n}(x_{ti} - \bar{x}_t)^2$, $\bar{x}_t = \frac{1}{n}\sum_{i=1}^{n} x_{ti}$, where n is the sample size. The mean and variance of Y_t are approximated by

$$\mu_Y = \ln \sigma^2 - \frac{1}{n-1} - \frac{1}{3(n-1)^2} + \frac{2}{15(n-1)^4}, \tag{1}$$

$$\sigma_Y^2 = \frac{2}{n-1} + \frac{2}{(n-1)^2} + \frac{4}{3(n-1)^3} - \frac{16}{15(n-1)^5}. \tag{2}$$

To detect an increase in the process variance, Crowder and Hamilton (1992) proposed an upper-sided EWMA chart based on

$$Q_t^+ = \max\{0, (1-\lambda)Q_{t-1} + \lambda Y_t\}, \tag{3}$$

where $0 < \lambda \leq 1$ and $Q_0^+ = 0$. The chart signals an out-of-control (OC) if Q_t^+ is greater than

$$h_Q^+ = L_Q \sqrt{\frac{\lambda}{2-\lambda}}\sigma_Y, \tag{4}$$

where L_Q^+ can be determined to achieve a desired in-control (IC) ARL. Similar to (3), in order to detect a decrease in the process variance, the lower-sided

EWMA chart can be based on

$$Q_t^- = \min\{0, (1-\lambda)Q_{t-1} + \lambda Y_t\}, \tag{5}$$

where $Q_0^- = 0$. The chart declares an OC signal if Q_t^- is less than

$$h_Q^- = -L_Q^- \sqrt{\frac{\lambda}{2-\lambda}}\sigma_Y, \tag{6}$$

where L_Q^- can be determined to achieve a desired IC ARL. The two-sided control chart consisting of a lower-sided CH chart and an upper-sided CH chart can be used together in order to detect an increase and a decrease in the process variance, simultaneously.

2.2 The EWMA SJ chart:

Based on definition of Y_t defined above, let $Z_t = (Y_t - \mu_Y|\sigma = 1)/\sigma_Y$, in order to detect an increase and decrease in the variance, define $Z_t^+ = \max[0, Z_t]$ and $Z_t^- = \min[0, Z_t]$, Shu and Jiang (2008) proposed an EWMA chart based on

$$W_t^+ = \lambda(Z_t^+ - \frac{1}{\sqrt{2\pi}}) + (1-\lambda)W_{t-1}^+, \quad t = 1, 2, \ldots, \tag{7}$$

where $W_0^+ = 0$ and $0 < \lambda \leq 1$. The chart declares an OC signal when W_t exceeds the upper control limit

$$h^+ = L^+ \sqrt{\frac{\lambda}{2-\lambda}}\sigma_{Z_t^+}, \tag{8}$$

where L^+ can be chosen to achieve a desired IC ARL. Analogously, in order to detect a decrease in the process variance, the EWMA chart can be based on

$$W_t^- = \lambda(Z_t^- + \frac{1}{\sqrt{2\pi}}) + (1-\lambda)W_{t-1}^-, \quad t = 1, 2, \ldots, \tag{9}$$

where $W_0^- = 0$. Subsequently, the lower control limit of the chart is given by

$$h^- = -L^- \sqrt{\frac{\lambda}{2-\lambda}}\sigma_{Z_t^-}, \tag{10}$$

where L^- can be determined to achieve a desired IC ARL and $\sigma_{Z_t^+} = \sigma_{Z_t^-}$. The two-sided control chart consisting of a lower-sided and an upper-sided SJ charts can be used together for detecting an increase and a decrease in the process variance, simultaneously.

2.3 The change point CUSUM chart (Acosta et al., 1999):

Let σ_1 be the process standard deviations that needs to be detected, then the two-sided procedure for detecting changes in the process variability can be expressed as

$$C_t^+ = \max\{0, C_{t-1}^+ + D_t^2 - \frac{n\sigma_1^2 \log \sigma_1^2}{\sigma_1^2 - 1}\}(\sigma_1 > 1), \tag{11}$$

$$C_t^- = \max\{0, C_{t-1}^- - D_t^2 + \frac{n\sigma_1^2 \log \sigma_1^2}{\sigma_1^2 - 1}\}(\sigma_1 < 1), \tag{12}$$

respectively, where $C_0^+ = C_0^- = 0$, $D_t^2 = \sum_{i=1}^n x_{ti}^2$, $t = 1, 2, \cdots$. The value C_t^+ is used to detect increase shifts in the process variance, while C_t^- is used to detect decrease shifts. The chart signals whenever C_t^+ or C_t^- exceeds its respective control limit, h_U or h_L. This chart will be denoted as CPC chart throughout the rest of this paper.

3 The new chart for monitoring the process variability

In this section, we will introduce our proposed chart that can be used to monitor the dispersion of a normal processes. We will show that our proposed charts are effective to detect both increases and decreases in process dispersion.

Let $\mathbf{x}_t = (x_{t1}, \ldots, x_{tn})$ denote a sample of size $n \geq 1$ taken on a quality characteristic x. The monitoring problems with $n > 1$ and $n = 1$ are usually referred to as group observations case and individual observations case, respectively. In industrial practice, sampling may be expensive, in such case, individual observation at sampling points is usually preferred. In what follows, we assume that the $\mathbf{x}_t$ for $t \geq 1$, the observations collected over time, come from the following process model

$$x_{ti} = \mu_t + \varepsilon_{ti}, \quad i = 1, \ldots, n, \quad t = 1, 2, \ldots, \tag{13}$$

where $\varepsilon_{t1}, \ldots \varepsilon_{ti}$ are identically and independently distributed (i.i.d) normal variables with mean zero and standard deviation σ. When the process is in-

control, $\mu = \mu_0$ and $\sigma = \sigma_0$. In this paper, we consider the Phase II case in which the IC μ_0 and σ_0 are assumed to be known, i.e., it is assumed that the IC data set used in Phase I is enough to estimate the parameters well. Without loss of generality, in the remainder of this paper, we assume $\mu_0 = 0$ and $\sigma_0 = 1$. Further assume that we are interested in detecting process variability, including the increase and decrease. When a process shift occurs, we assume $\sigma \neq 1$.

For a given sample $\mathbf{x}_t$, consider the following hypothesis test

$$H_0 : \sigma = 1 \longleftrightarrow H_1 : \sigma \neq 1. \tag{14}$$

Then, the generalized likelihood ratio statistic can be obtained as follows

$$l_t = n(s_t^2 - \ln s_t^2 - 1), \tag{15}$$

where $s_t^2 = \sum_{j=1}^{n} x_{tj}^2/n$. It can be seen that $l_t \xrightarrow{\mathcal{L}} \chi^2(2)$ as $n \to \infty$. A large l_t leads to reject the null hypothesis.

Note that the function $f(z) = z - \ln z$ is monotonically increase (decrease) when $z > 1$ $(0 < z < 1)$ and attains its minimum at $z = 1$. Hence, the testing statistics l_t will be sensitive to both the increase and decrease in variance. Unlike other test statistics in the literature, l_t is a likelihood ratio derived under the setting in which the process variance may change, and thus naturally adapts to be sensitive to various types of shifts. For simplicity, the coefficient n and the constant term -1 can be ignored, so we have

$$LR_t = s_t^2 - \ln s_t^2. \tag{16}$$

In order to detect small or moderate shifts effectively, we incorporate the EWMA procedure into the construction of LR_t. First, let

$$u_t = \lambda s_t^2 + (1 - \lambda)u_{t-1}, \tag{17}$$

where $u_0 = 1$ and λ is the smoothing parameter satisfying $0 < \lambda \leq 1$. In general, a smaller λ leads to a quicker detection of smaller shifts. Then, substitute u_t for s_t^2 in (16) and obtain the following charting statistics

$$ELR_t = u_t - \ln(u_t), \quad t = 1, 2, \ldots, \tag{18}$$

An alarm is trigged when $ELR_t > h$, where $h > 0$ is chosen to achieve a specified IC ARL. This chart is denoted as ELR chart. It can be seen that our ELR chart still works when $n = 1$ due to the definition of u_t.

Most of the existing charts need two one-sided charts to detect the process variance change simultaneously, one is to detect an increase and another one is to detect a decrease, so two individual control limits should be specified. However, for the ELR chart, only one control limit is needed, so it is more convenient in the practical application than some other charts.

Sometimes, we are interested in detecting process deteriorations in terms of increase, i.e., $\sigma > 1$, in order to further improve the detection performance of the control chart, define:

$$u_t^+ = \max(1, \lambda s_t^2 + (1 - \lambda)u_{t-1}^+), \tag{19}$$

with $u_0^+ = 1$ as the initial value. Clearly, the reset of the EWMA statistic to one whenever it is less than one can ameliorate the inertia problem of the EWMA statistic. Then, an upper-sided ELR chart aiming at detecting an increase in the variance is defined as:

$$ELR_t^+ = u_t^+ - \ln u_t^+, \quad t = 1, 2, \ldots. \tag{20}$$

Similarly, in order to detect a decrease in the variance, i.e., $\sigma < 1$, define:

$$u_t^- = \min(1, \lambda s_t^2 + (1 - \lambda)u_{t-1}^-), \tag{21}$$

with $u_0^- = 1$ as the initial value and then, a lower-sided ELR chart aiming at detecting a decrease in the variance is defined as:

$$ELR_t^- = u_t^- - \ln u_t^-, \quad t = 1, 2, \ldots. \tag{22}$$

The ELR chart signals whenever ELR_t^+ or ELR_t^- exceeds its respective control limit, h_U or h_L.

One can expect that the two one-sided charts based on equation (20) and (22) will be more effective than the ELR chart based on equation (18) if the aim is to detect the increase and decrease in the process variance.

4 Run length distribution of the proposed chart

In this section, we discuss the run length distribution of the proposed chart. Run length is the number of observations until the first OC signal is triggered by the control chart. Figure 1 plots the IC and OC run-length probability mass function (PMFs) for the upper-sided and lower-sided ELR charts, respectively. The run-length distributions of the SJ chart and the CPC chart are also plotted for comparison. In this comparison, the two EWMA-type charts are based on $\lambda = 0.1$ and n $= 5$ and for the CPC chart, $\sigma_1 = 1.2$ and 0.8 are used in Equation (11) and (12) for monitoring the process increase and decrease in dispersion, respectively. We plot the PMFs for different charts in Figure 1 when the run length $T \leq 50$.

Concerning the increasing case, as can be seen from Figure 1(a), in the IC situation, the probability of a false alarm triggered on the ELR chart is lower than those of the SJ chart and the CPC chart at short run length $T < 15$, and higher at run length $T > 15$. In the OC situation ($\sigma = 1.2$), as shown in Figure 1(b), compared with SJ chart, the ELR chart has a slightly higher signal probability at very short run length $T < 5$, and has similar performance compared with the CPC chart, and slightly higher signal probability at run length $T > 5$. Also we can see that the ELR chart almost has similar performance compared with the CPC chart.

Concerning the decreasing case, as can be seen from Figure 1(c), in the IC situation, the probability of a false alarm triggered on the ELR chart is much lower than those of the SJ and CPC charts at short run length, $T < 15$, and much higher at run length, $T > 15$. In the OC situation ($\sigma = 0.8$), as shown in Figure 1(d), the CPC chart has a slightly higher signal probability than the ELR chart at very short run length, $T < 10$, and slightly smaller signal probability at run length $10 < T < 25$, but the difference is negligible. When $T > 25$, both of the charts have similar run length distribution. On the other hand, it can be seen that the run length distribution is significantly different between the ELR chart and the SJ chart. The ELR chart has a much higher signal probability than the SJ chart at short run length $8 < T < 20$, but much smaller signal probability at run length $T > 20$. The superior signal probabilities of the ELR chart at short run lengths are very attractive for early detection of process-dispersion changes.

To gain more insight into the run length distribution of the ELR, CPC and SJ charts, we also present OC run length cumulative distribution function (CDFs) of these charts concerning the increasing and decreasing cases in Figure 1(e) and (f), respectively. It can be observed that concerning the increasing case, the CDF of the ELR chart is slightly higher than the SJ chart and the CDF of the CPC chart is slightly higher than the ELR chart. Concerning the

decreasing case, the CDF of the ELR chart is much higher than the SJ chart when $T > 7$ and slightly lower than the CPC chart when $T < 20$. Note that this high probability indicates that the shifts in the process variance will be detected quickly with high probability.

The overall conclusion is that the ELR chart has high probability at shorter run lengths, which implies that the ELR chart is a useful tool for practitioners when taking into account its performance in detecting variance shifts.

5 Design of the ELR chart

The design approach recommended by Crowder and Hamilton (1992) will be followed in this paper for the ELR chart. The approach involves the joint choice of λ and h that yields a desired zero-state IC ARL at the nominal variability ($\sigma = 1$) and also yields the smallest zero-state OC ARL for a specified change in the process standard deviation. The zero-state OC ARL performance assumes that the process is OC when the initial subgroup from the process is obtained. The steady-state OC ARL performance assumes that the process is initially IC but shifts to an OC state at the change point.

For a target OC σ and a fixed sample size n, we search the corresponding values of h with a wide range values of λ ($\lambda = 0.01, \cdots, 0.99, 1.0$) to yield the desired zero-state IC ARL. The pair (λ, h) will be considered to be optimal if among all the possible combinations of λ and h, which produces the smallest zero-state OC ARL at the target OC σ.

Tables 1-3 present a list of optimal parameters of an upper-sided ELR chart based on Equation (20) and lower-sided ELR chart based on Equation (22) when $n = 1$, 5 and 10, respectively, for providing a desired IC ARL. These parameters are adequate for most practical purposes and are obtained using a numerical search method through the Monte Carlo simulation.

Examination of Tables 1-3 indicates that, for a fixed IC ARL, the optimal value of λ increases as the target dispersion changes increase. Therefore, as expected, a small value of λ is more sensitive to small changes while a large value of λ is more sensitive to large changes. Moreover, the optimal λ values for detecting a specific dispersion change may be different when n is different. For example, when the sample size increases from $n = 5$ to 10, the optimal λ value of the upper-sided ELR chart increases from 0.08 to 0.13 in order to efficiently detect a dispersion change of 20% with an IC ARL of 200.

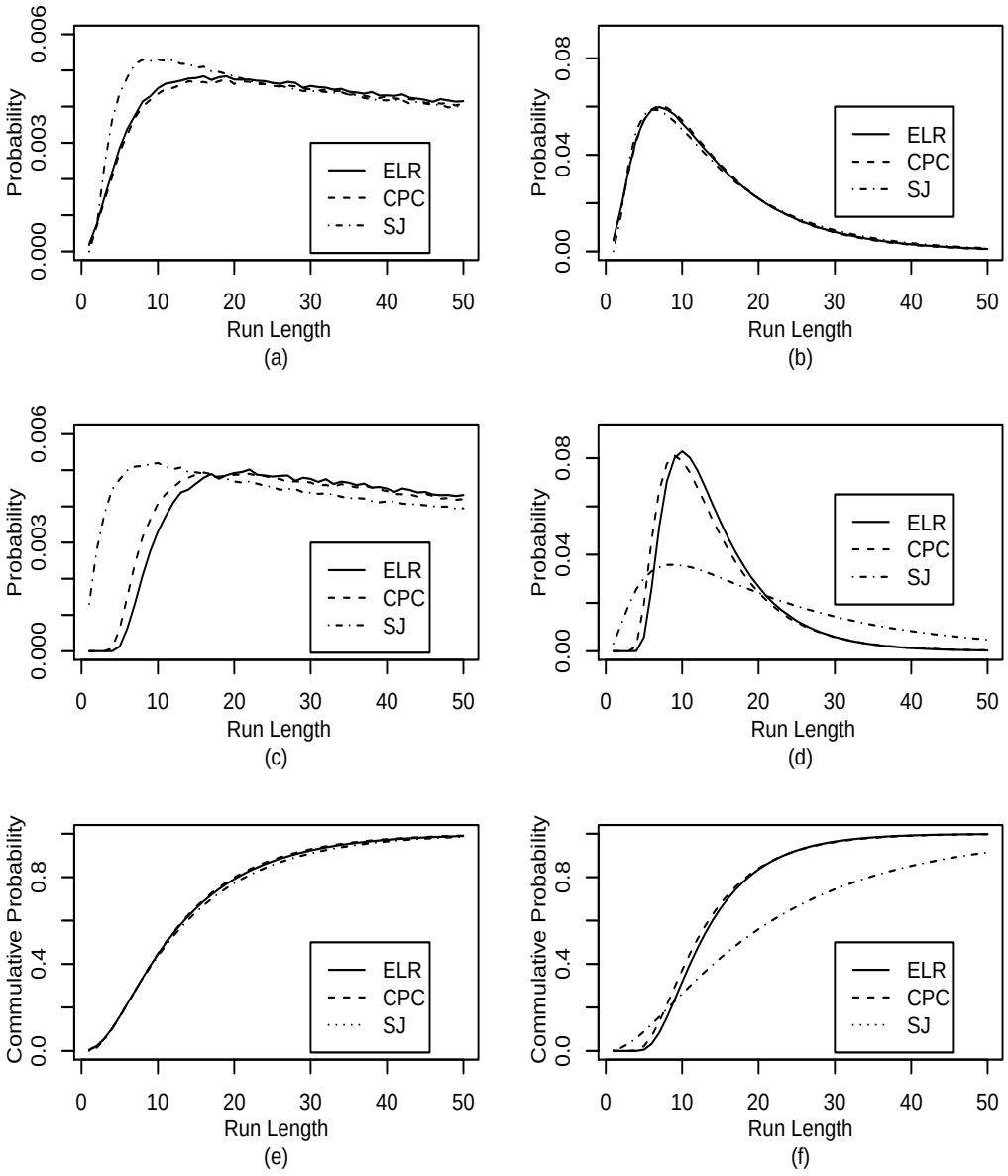

Fig. 1. One-sided run length PMFs and CDFs of the ELR, CPC and SJ charts when $\lambda = 0.1, n = 5$ and IC ARL=200. (a) upper-sided IC run length PMFs; (b) upper-sided OC run length PMFs when $\sigma = 1.2$; (c) lower-sided IC run length PMFs; (d) lower-sided OC run length PMFs when $\sigma = 0.8$; (e)upper-sided OC run length CDFs when $\sigma = 1.2$; (f) lower-sided OC run length CDFs when $\sigma = 0.8$

6 Performance comparison

To evaluate the sensitivity against shifts in the process standard deviation, we assume in our comparisons that the process mean does not change. The discussions will be based on the subgroup size of $n = 5$. The cases based on other different sample sizes can be similarly discussed, which provide qualita-

tively the same conclusions. For simplicity, we only present the results based on $n = 5$ in this paper.

6.1 Comparison of upper-sided EWMA-type charts

First, we compare three upper-sided EWMA-type charts, i.e., the ELR chart, the SJ chart and the CH chart when there is an increase in the process standard deviation. Each chart is calibrated so that the IC ARL is approximately equal to 200. The ARL values are obtained using at least 200,000 run length simulations. A FORTRAN computer program is coded for these simulations. In each independent run, the run length for that run is recorded as the number of simulated samples that must be observed until the control chart signals. The estimated ARL is the average of these independent run lengths. The steady-state OC ARLs are obtained when the monitoring statistics are processed for 100 in-control observations before the run lengths are accumulated to signal. If a signal occurred before those first 100 in-control observations, then that particular run was discarded and a new set of 100 samples were generated.

Table 4 and Table 5 present the zero-state and steady-state ARL values for various shifts in the process mean and different λ when $n = 5$. We also plot the zero-state and steady-state ARLs of the three charts at a given percent increasing change in the process standard deviation from 10% to 100% for $\lambda = 0.05, 0.1, 0.2$ and 0.3 for illustration in Figures 2-3.

From Table 4 and Table 5, it can be observed that for detecting the increase in the variance, for a given value of λ, the zero-state OC ARL values of the ELR chart are almost uniformly smaller than those of the SJ chart, except for the case when $\sigma = 1.1$ and $\lambda < 0.9$. We also notice that the ELR chart almost always has smaller steady-state ARL values. When $\lambda = 1$, the ELR chart performs much better than the SJ chart, and in this case, the SJ chart and the CH chart reduce to an upper-sided Shewhart chart of Z_t and thus show essentially the same performance. On the other hand, the ELR chart consistently produces smaller ARL than the CH chart and the difference is more significant for the smaller λ. For instance, when $\lambda = 0.1$ and $\sigma = 1.1$, the OC ARL in this case is 35.29 for the ELR chart and 44.19 for the CH chart. However, when $\lambda = 0.9$ and $\sigma = 1.1$, the OC ARL is 59.16 for the ELR chart and 62.38 for the CH chart. In this case, the difference is small.

Comparing Table 4 with Table 5, it is also observed that for the ELR chart and the CH chart, the steady-state OC ARL is notably smaller than the zero-state OC ARL when the process variance increases, and the difference is more significant for the smaller λ. As for the SJ chart, the steady-state OC ARL is larger than the zero-state OC ARL at an increase in the process variance

when $\lambda = 0.05$ and 0.1, but the direction of the discrepancy is not clear and they are not significantly different as $\lambda \geq 0.2$.

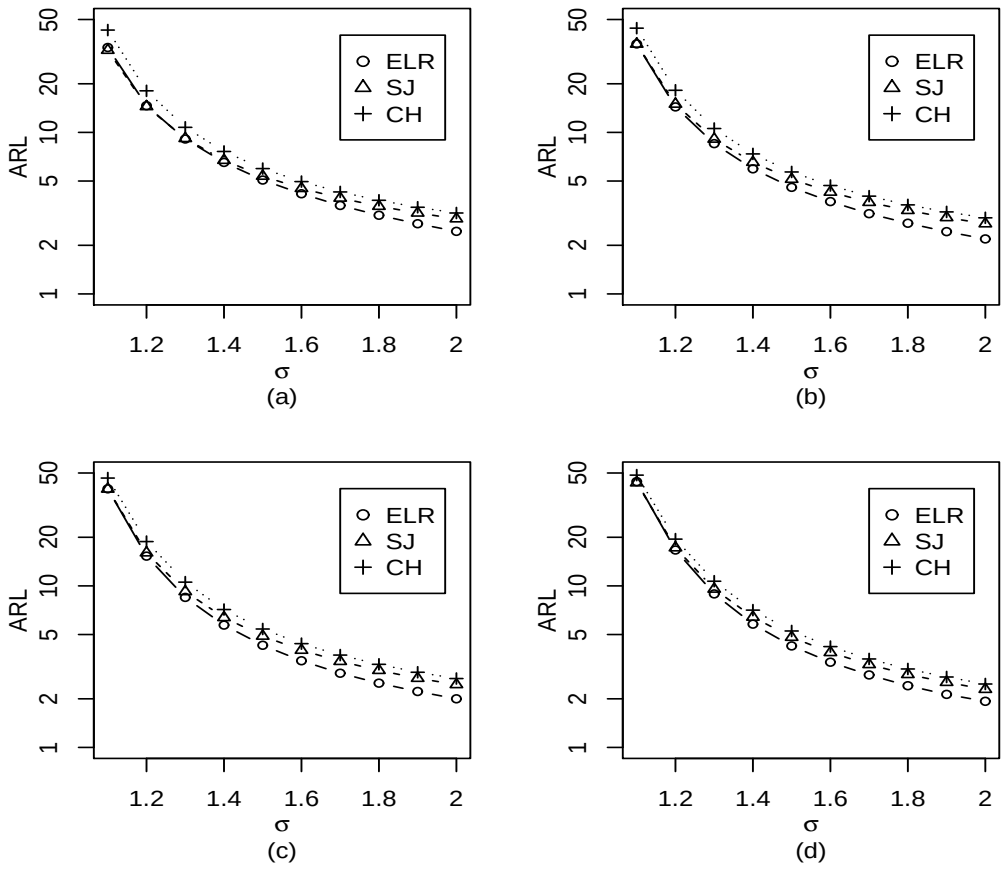

Fig. 2. The zero-state OC ARL for the ELR, CH and SJ charts when the process variance increases. (a) $\lambda = 0.05$; (b) $\lambda = 0.1$; (c) $\lambda = 0.2$; (d) $\lambda = 0.3$

The standard deviation of the run length (denoted as SDRL) is usually used as another measure to evaluate the performance of control charts. The smaller the values of SDRL, the better the performance of a control chart. The SDRLs for the three charts are summarized in Table 6 when $\lambda = 0.1$ and $\lambda = 0.3$. It can be seen that the ELR chart is almost always more under dispersed than the other two charts. For instance, when $\lambda = 0.3$ and $\sigma = 1.2$, the zero-state SDRL of the ELR chart is 14.84, while for the SJ and the CH charts, the corresponding values are 15.06 and 17.32, respectively. We also conduct some simulations for other choices of sample size, λ and IC ARL, the preceding findings still hold. The simulation results show that the ELR chart has quite a satisfactory performance in other cases as well.

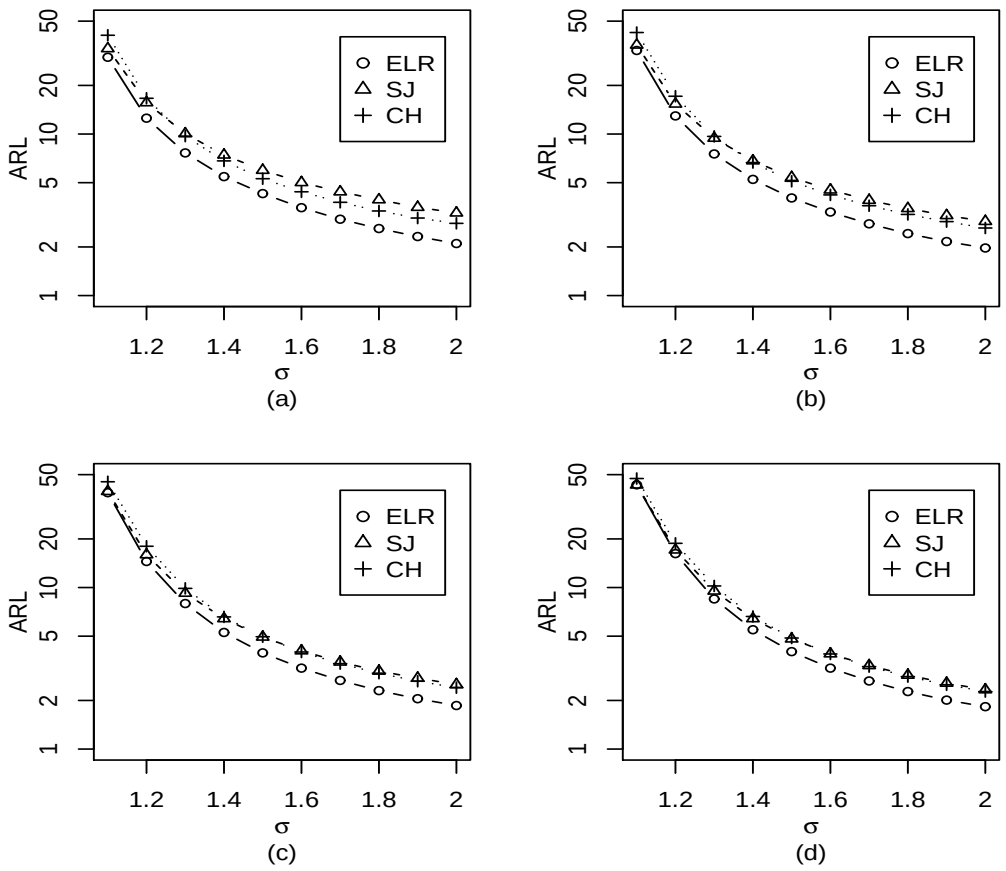

Fig. 3. The steady-state OC ARL for the ELR, CH and SJ charts when the process variance increases. (a) $\lambda = 0.05$; (b) $\lambda = 0.1$; (c) $\lambda = 0.2$; (d)$\lambda = 0.3$

6.2 Comparison of lower-sided EWMA-type charts

Second, the zero-state and steady-state OC ARL comparison for monitoring decreases in process dispersion is tabulated in Table 7 and Table 8. (We plot the zero-state and steady-state ARLs of the three charts at a given percent decreasing change in the process standard deviation from -10% to -50% for $\lambda = 0.05, 0.1, 0.2$ and 0.3 for illustration in Figures 4-5.) It can be seen that the ELR chart with small λ ($\lambda \leq 0.3$) is more efficient at detecting small to moderate shifts than the SJ chart, while the SJ chart is more efficient at detecting large shifts. For instance, when $\lambda = 0.2, \sigma = 0.8$, the OC ARL in this case is 13.51 for the ELR chart and 30.78 for the SJ chart. Also notice that the ELR chart with large λ ($\lambda > 0.3$) always outperforms the SJ chart. On the other hand, the ARL values of the ELR chart are uniformly smaller than those of the CH chart. The performance improvement of the ELR chart is profound especially when λ is small. Moreover, for small λ values, the difference in the ARLs between the ELR and the other two charts becomes significant when the degree of decrease in the variance is small.

It can be observed that when the aim is to monitor decreases in variability, the improvement achieved in terms of ARL performance by the ELR chart is considerably greater than those for monitoring increases. The use of the $\ln S^2$ statistic or other transformed statistics result in improved performance but they are not the best choice. In addition, it is not always desirable to monitor a process using a transformed scale.

The SDRLs concerning the decreasing case of the three charts are presented in Table 9. From this Table, we can see that the SDRLs of the ELR chart are always much smaller than the other two charts. For instance, when $\lambda = 0.3$ and $\sigma = 0.8$, the zero-state SDRL of the ELR chart is 12.92, while for the SJ and the CH charts, the corresponding values are 36.32 and 27.78, respectively. Again, the ELR chart is always more under dispersed than the other two charts.

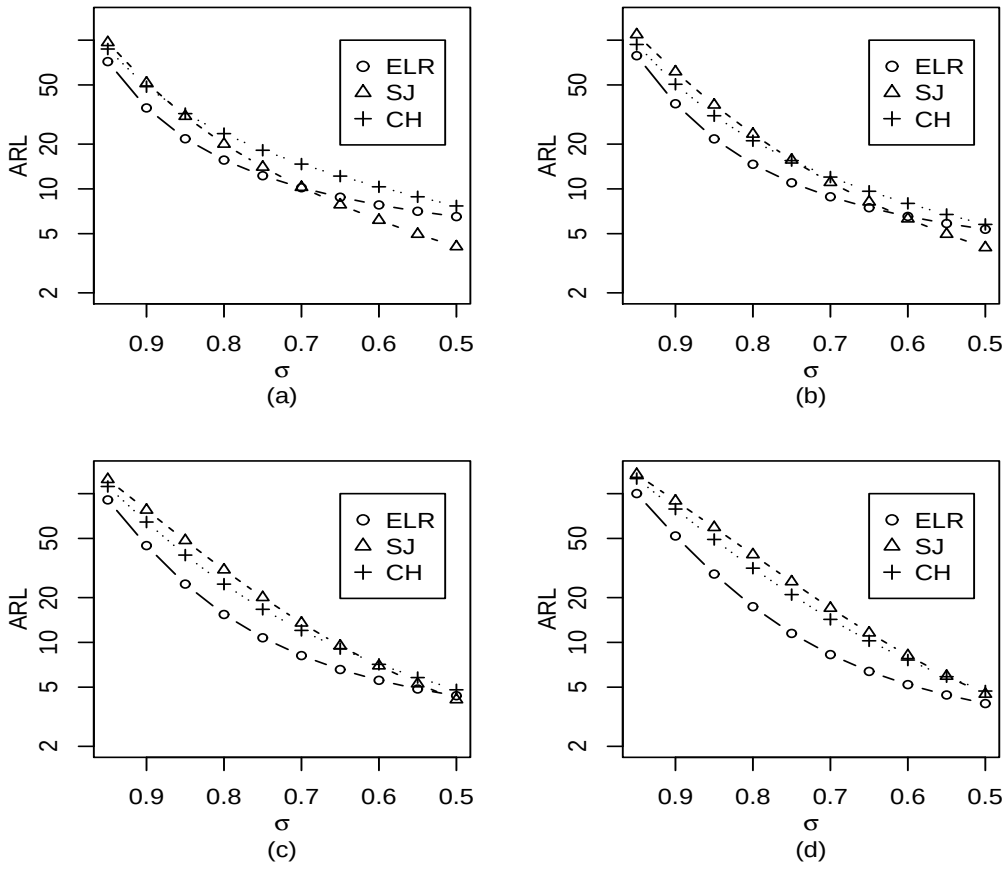

Fig. 4. The zero-state OC ARL for the ELR, CH and SJ charts when the process variance decreases (a)$\lambda = 0.05$; (b)$\lambda = 0.1$; (c)$\lambda = 0.2$; (d)$\lambda = 0.3$

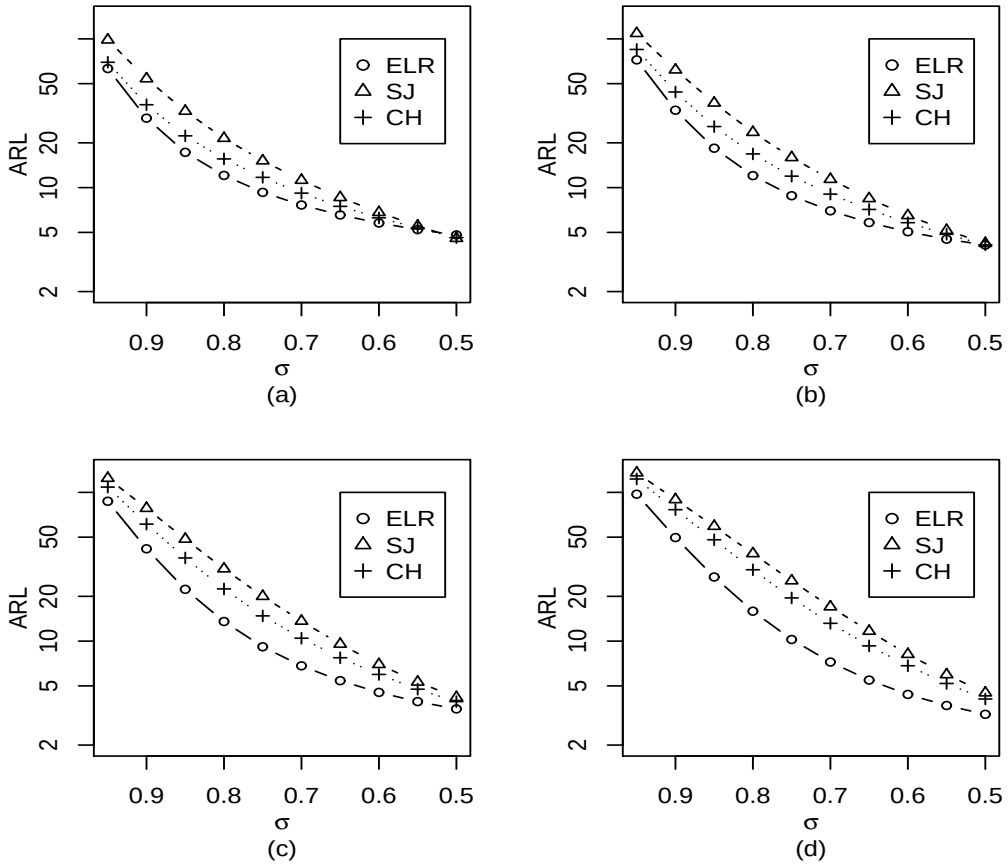

Fig. 5. The steady-state OC ARL for the ELR, CH and SJ charts when the process variance decreases (a)$\lambda = 0.05$; (b)$\lambda = 0.1$; (c)$\lambda = 0.2$; (d)$\lambda = 0.3$

6.3 Comparison with the corresponding optimal parameters

Note that the same value of λ is used for comparison in Tables 4-9. However, the same λ value may not be optimal for these three EWMA-type charts for detecting a particular increase in the process standard deviation. For this reason, Table 10 further compares the optimal ARL performance among the three EWMA-type charts for detecting a 20% increase and a 40% increase in the process standard deviation in terms of zero-state and steady-state ARL, respectively. Moreover, besides the three EWMA-type charts, another technique compared is the CPC chart based on Equation (11). In this case, $\sigma_1 = 1.2$ and 1.4 are considered, and the corresponding control limits are 18.5 and 13.3, respectively. According to Table 2 in Shu and Jiang (2008), the corresponding optimal parameters for the SJ chart are $(\lambda, L_W^+) = (0.03, 1.27)$ and $(0.2, 2.27)$, and for the CH chart, the corresponding optimal parameters are (λ, L_Q^+)=(0.05, 1.06) and (0.32, 1.61). From Table 2, the corresponding optimal parameters for the ELR chart are (λ, h^+)=(0.08, 1.0445) and (0.21, 1.1545), respectively.

It can be concluded from Table 10 that in terms of zero-state ARL, the SJ chart performs better than the other charts at the specified magnitude of increase in the process standard deviation when $\sigma_{opt} = 1.2$. However, when the shift in the variance differs from σ_{opt}, for instance, $\sigma > \sigma_{opt}$, the CPC chart has the best performance, but the difference between the ELR chart and the CPC chart is small. When σ_{opt} is 1.4, the CPC chart and the ELR chart almost have the same performance and they consistently outperform the other two charts. On the other hand, in terms of the steady-state ARL, the OC ARLs of the ELR charts are uniformly smaller than those of the other three charts but the differen between the ELR chart and the CPC chart is negligible.

Similarly, Table 11 further compares the optimal ARL performance among the four charts for detecting a 20% decrease and a 40% decrease in the process standard deviation, respectively. The corresponding optimal parameters for the SJ chart are $(\lambda, L_W^-) = (0.04, 2.01)$ for these two cases. As for the CH chart, the corresponding optimal parameters are (λ, L_Q^-)=(0.1, 3.72) and (0.2, 3.67). From Table 2, the corresponding optimal parameters for the ELR chart are (λ, h^-)=(0.1, 1.0559) and (0.36, 1.2687), respectively. It can be concluded that in terms of zero-state ARL, the CPC chart performs better than the other charts at the specified magnitude of decrease in the process standard deviation, while, in terms of steady-state ARL, the ELR chart performs better than the other charts.

6.4 Comparison of two-sided charts

Next, we consider the performance of these charts for monitoring decrease and increase in process variability simultaneously. It should be noted that for the ELR chart based on Equation (18), only one control limit is needed in the design procedure in this situation. While, for each of the other three two-sided control charts, an upper control limit and a lower control limit should be specified. We use 200,000 Monte Carlo simulations to find the individual control limit value for each of the two one-sided charts with equal individual zero-state IC ARL (nearly 400) so that the overall zero-state IC ARL of the two-sided chart is approximately equal to 200. The three EWMA-type charts are designed with λ=0.05, 0.1, 0.2, 0.3 and the two-sided CPC chart with (a, b) (denoted as $\text{CPC}_{(a,b)}$) stands for the chart which is prespecified to respond quickly to the change of $\sigma_1 = a$ in Equation (12) (for detecting a decrease) and $\sigma_1 = b$ in Equation (11) (for detecting an increase) in the process dispersion, respectively. The CPC charts with (a, b)=(0.9, 1.1), (0.8, 1.2), (0.7, 1.3) and (0.6, 1.4) (denoted as CPC_1, CPC_2, CPC_3, and CPC_4, respectively) are compared with EWMA-type charts with $\lambda = 0.05$, 0.1, 0.2 and 0.3, respectively. The steady-state OC ARL simulation results based on $n = 5$ are summarized in Table 12.

According to the results in Table 12 and Figure 6, it can be seen that the ELR chart always performs best among the three EWMA-type charts. Compared with the CPC chart, concerning the increasing case, the ELR chart performs better than the CPC chart, while concerning the decreasing case, the CPC chart slightly outperforms the ELR chart. When the process variance decreases, the CH chart does better than the SJ chart and the SJ chart turned out to be ARL-biased when $\sigma = 0.95$, i.e., the OC ARL is larger than the IC ARL. When the variance increase, the SJ chart does better than the CH chart.

The overall conclusion that can be obtained from Tables 4-12 is that the ELR chart generally has the satisfactory detection performance for various changes in the process variance. This shows that the ELR chart is quite a useful alternative tool for practitioners by taking into account its performance of detecting various variance shifts.

It should be noted that the numerical method used above can only find the approximate optimal values because the true optimal λ may occur at the value different from the prespecified interval (0.01, 1). For a fixed IC ARL, smaller λ gives smaller OC ARL, but, when too small a λ is used, the standard deviation of the run-length (denoted as SDRL) is usually very large for a control chart. For example, for the SJ chart, when $\lambda = 0.01$, the SDRL associated with IC ARL=200 equals 250.2, which is much larger than the counterpart of the value 202.8 when $\lambda = 0.04$. Large variability of run-length distribution at small value of λ usually prevents the practitioner from choosing it as the smoothing constant to use in practice. This is why we choose $\lambda = 0.04$ as the optimal parameter for the SJ chart in the comparison for detecting a decrease in the dispersion.

7 A real data example

In this section, we demonstrate our proposed methodology by a real data example which contains a data set consisting of measurements of the inside diameter of the cylinder bores in an engine block. Chen et al. (2001) and Zhang et al. (2011) also used this data set to show the implementation of their charts for monitoring the process. The original data set can be found in Chen et al. (2001). A Phase I dataset of $m = 35$ samples, each having sample size $n = 5$, have been collected. First, we use the grand average of the preliminary data to estimate the process mean μ and use $\frac{\bar{S}}{c_4}$ to estimate the process variance σ, where $\bar{S} = \frac{1}{m}(S_1 + \cdots + S_m)$ is the average of the sample standard deviations, and $S_i^2 = \frac{1}{n-1}\sum_{j=1}^{n}(x_{ij} - \bar{x}_i)^2$ is the i-th sample variance.

The process mean and variance are estimated from the data set and we have

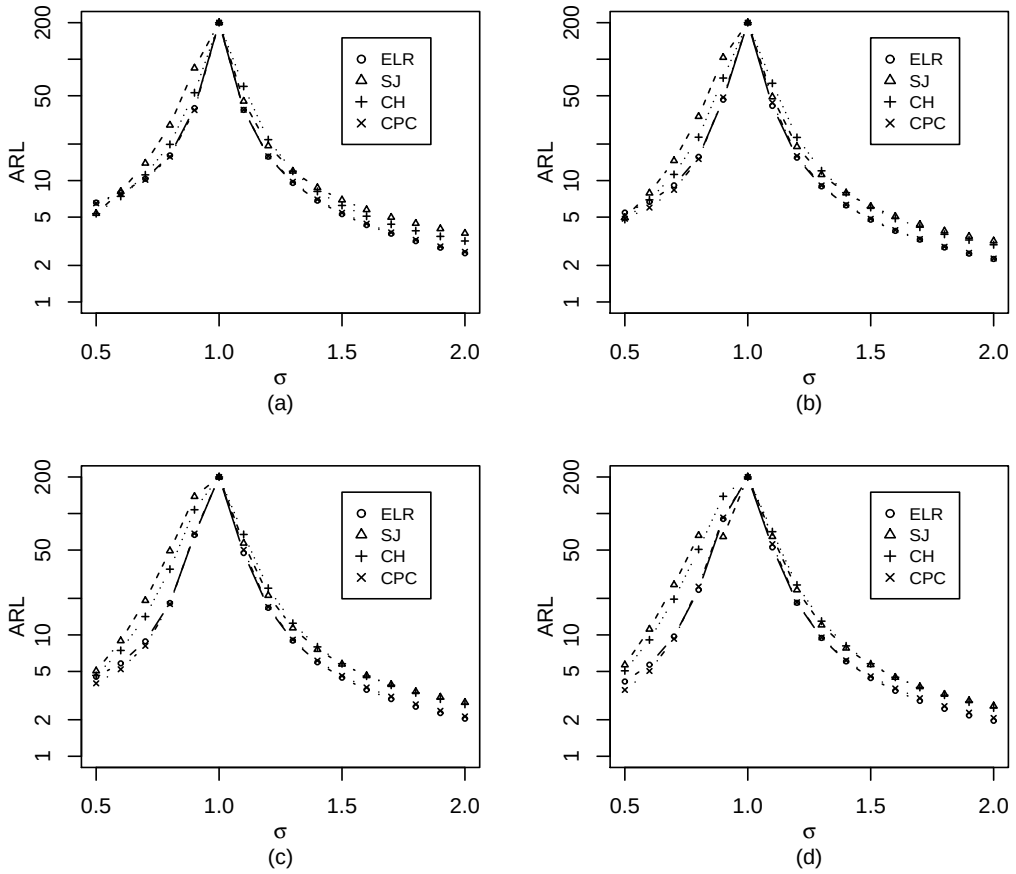

Fig. 6. The two-sided steady-state OC ARL for the ELR, CH, SJ and CPC charts when the process variance increases or decreases.

$\hat{\mu} = 200.251$ and $\hat{\sigma} = 3.306$. In this example, the in-control ARL is chosen to be 200 and the corresponding control limit is 1.0445. The chart is shown as a plot in Figure 7. We can see that the curve has a suddenly increase from sample 6 and this point exceeds the control limit, which is related to the process variance. When this point is removed, we obtain $\hat{\mu} = 200.22$ and $\hat{\sigma} = 3.1$, and our second ELR chart is given as a plot in Figure 8. The OC signal is triggered at the original sample 16 and this sample is also related to the process variance. When these two samples are removed, we obtain $\hat{\mu} = 200.23$ and $\hat{\sigma} = 2.93$, and our third ELR chart is given as a plot in Figure 9. It shows that there is no point falling outside the control limit.

8 Conclusions

In this paper, we propose a new method for monitoring the process variance including the increase and decrease by using a single chart. The proposed scheme integrates the EWMA procedure with the GLR statistics. The main

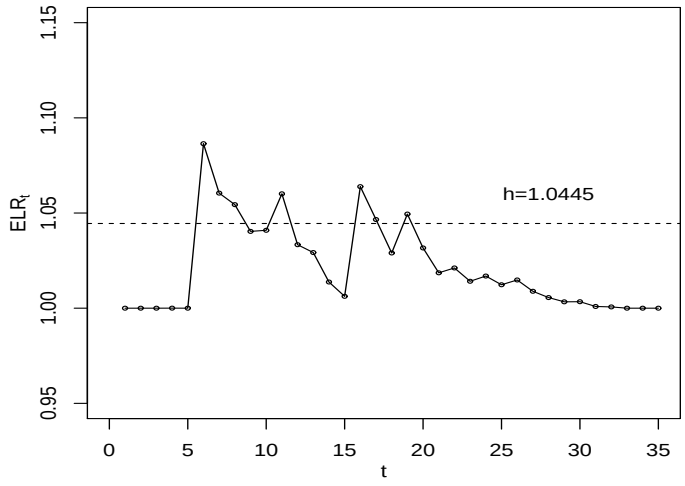

Fig. 7. The ELR chart for the cylinder data with the dashed horizontal line indicating its control limit.

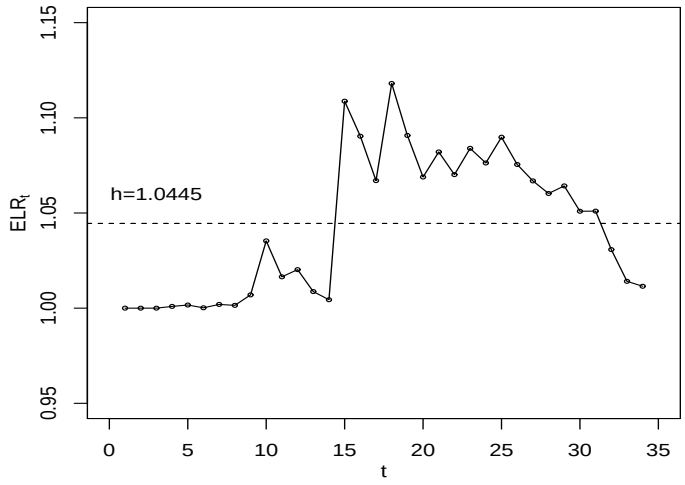

Fig. 8. The ELR chart for the cylinder data with the dashed horizontal line indicating its control limit after removing sample 6.

advantages of this control chart are: (1) it can be easily designed and constructed; (2) it can effectively detect the decrease in variability; (3) it is able to handle the case that the sample size is one, which is also very important in many practical applications. Since the ELR chart for process dispersion performs better than most of the other procedure for detecting both increases and decreases in process dispersion, we recommend its use. We have provided optimal parameters that can be used as a design aid in selecting specific parameter

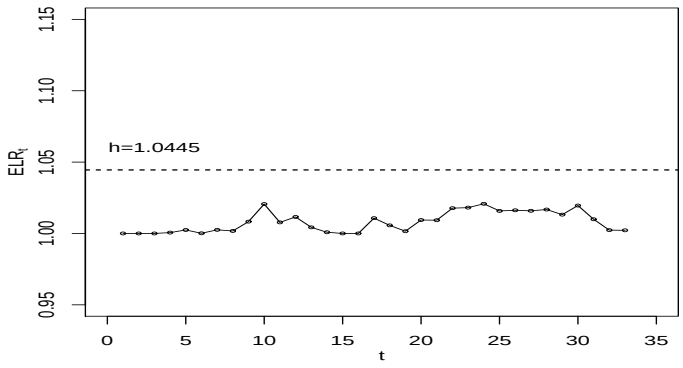

Fig. 9. The ELR chart for the cylinder data with the dashed horizontal line indicating its control limit after removing samples 6 and 16.

values for this process dispersion control chart.

It is worth noting that the ELR chart is based on independent observations, so, the chart is expected to be affected by autocorrelation. In addition, the new chart is based on the normality assumption, and thus its robustness deserves further investigation.

Acknowledgement

The authors are grateful to the editor and the anonymous referee for their valuable comments that have vastly improved this paper. This research is supported by the Natural Science Foundation of China Grant 11101198, 11201246, 11371202, 11131002, the start-up funding at Liaoning University and the RFDP of China Grant 20110031110002.

References

Abbas, N., Riaz, M., Does, R. J. M. M., 2013a. CS-EWMA chart for monitoring process dispersion. Quality and Reliability Engineering International, 29, 653-663.

Abbas, N., Riaz, M., Does, R. J. M. M, 2013b. Memory-Type control charts for monitoring the process dispersion. Quality and Reliability Engineering International, DOI: 10.1002/qre.1514.

Abbasi, S. A., Miller, A., 2013. MDEWMA chart: an efficient and robust alternative to monitor process dispersion. Journal of Statistical Computation and Simulation, 83(2), 247-268.

Abbasi, S. A., Riaz, M., Miller, A., 2012. Enhancing the performance of CUSUM scale chart. Computers and Industrial Engineering. 63(2), 400-409.

Acosta-Mejia, C. A., Pignatiello, J. J., Rao, B. V., 1999. A comparison of control charting procedures for monitoring process dispersion. IIE Transactions, 31, 569-579.

Ahmad, S., Abbasi, S. A., Riaz, M., Abbas, N., 2014. On efficient use of auxiliary information for control charting in SPC. Computers and Industrial Engineering, 67, 173-184.

Ahmad, S. Riaz, M., Abbasi, S. A., Lin, Z. Y., 2013. On monitoring process variability under double sampling scheme. International Journal of Production Economics, 142(2), 388-400.

Alt, F. B., 1984. Multivariate quality control. In S. Kotz, N. L. Johnson, & C. R. Read (Eds.), The encyclopedia of statistical sciences. New York: Wiley, 110-122.

Barbosa, E. P., Gneri, M. A., Meneguetti, A., 2013. Range control charts revisited: simpler tippett-like formulae,its practical implementation, and the study of false alarm. Communications in Statistics - Simulation and Computation, 42(2), 247-262.

Castagliola, P., 2005. A new S^2-EWMA control chart for monitoring the process variance. Quality and Reliability Engineering International, 21, 781-794.

Castagliola, P., Celano, G., Fichera, S., Giuffrida, F., 2007. A variable sampling interval S^2-EWMA control chart for monitoring the process variance. International Journal of Technology Management 37, 125-146.

Castagliola, P., Celano, G., Fichera, S., Giuffrida, F., 2009. A new CUSUM S^2 control chart for monitoring the process variance. Journal of Quality in Maintenance Engineering, 15(4), 344-357.

Castagliola, P., Maravelakis, P., 2009. An EWMA chart for monitoring the process standard deviation when parameters are estimated. Computational Statistics and Data Analysis, 53, 2653-2664.

Chang, T. C., Gan, F. F. (1994). Optimal designs of one-sided EWMA charts for monitoring a process variance. Journal of Statistical Computation and Simulations, 49, 33-48.

Chen, G., Cheng, S. W., Xie, H., 2001. Monitoring process mean and variability with one EWMA chart. Journal of Quality Technology, 33, 223-233.

Collani, E. V., Sheil, J., 1989. An approach to controlling process variability. Journal of Quality Technology, 21, 87-96.

Crowder, S. V., Hamilton, M. D., 1992. An EWMA for monitoring a process standard deviation. Journal of Quality Technology, 24, 12-21.

Huang, H., Chen, F., 2005. A synthetic control chart for monitoring process dispersion with sample standard deviation. Computers and Industrial Engineering, 49, 221-240.

Human, S. W., Chakraborti, S., Smit, C. F., 2010. Shewhart-type control charts for variation in phase I data analysis. Computational Statistics and Data Analysis, 54, 863-874.

Huwang, L., Huang, C. J., Wang, Y. H. T., 2010. New EWMA control charts for monitoring process dispersion. Computational Statistics and Data Analysis, 54, 2328-2342.

Knoth, S., 2006. Computation of the ARL for CUSUM-S2 Schemes. Computational Statistics and Data Analysis, 51, 499-512.

Montgomery, D. C., 2009. Introduction to Statistical Quality Control. 6th Ed. New York: John Wiley & Sons.

Nazir, H.Z., Riaz, M., Does, R. J. M. M., 2013. Robust CUSUM control charting for process dispersion. Quality and Reliability Engineering International. DOI: 10.1002/qre.1596.

Nazir, H.Z., Schoonhoven, M., Riaz, M., Does, R. J. M. M., 2013. How to set up a robust shewhart control chart for dispersion?, Quality Engineering, 26(1), 130-136.

Nelson, L. S., 1990. Monitoring reduction in variation with a range chart. Journal of Quality Technology, 22, 163-165.

Ng, C. H., Case, K. E. (1989). Development and evaluation of control charts using exponentially weighted moving averages. Journal of Quality Technology, 21, 242-250.

Page, E. S., 1963. Controlling the standard deviation by CUSUM and warning lines. Technometrics, 5, 307-315.

Riaz, M., 2008. A dispersion control chart. Communication in Statistics: Simulation and Computation 37, 1239-1261.

Riaz, M., 2013. On enhanced interquartile range charting for process dispersion. Quality and Reliability Engineering International, DOI: 10.1002/qre.1598.

Riaz, M., Abbasi, S. A., Ahmad, S., Zaman, B., 2014. On efficient phase II process monitoring charts. International Journal of Advanced Manufacturing Technology. 70, 2263-2274.

Riaz, M., Saghir, A., 2009. A mean deviation based approach to monitor process variability. Journal of Statistical Computation and Simulation, 79 (10), 1173-1193.

Schoonhoven, M., Does, R. J. M. M., 2012. A robust standard deviation control chart. Technometrics 54(1), 73-82.

Schoonhoven, M., Riaz, M., Does, R. J. M. M., 2011. Design and analysis of control charts for standard deviation with estimated parameters, Journal of Quality Technology, 43(4), 307-333.

Shu, L., Jiang, W., 2008. A new EWMA chart for monitoring process dispersion. Journal of Quality Technology, 40, 319-331.

Tuprah, K., Ncube, M., 1987. A comparison of dispersion quality control charts. Sequential Analysis, 6(2), 155-163.

Zhang, J., Zou, C., Wang, Z., 2011. An adaptive Shiryaev-Roberts procedure for monitoring dispersion. Computers and Industrial Engineering, 61, 1166-1172.

Table 1
Optimal parameters of one-sided ELR charts based on sample size of n=1

	In-Control ARL				
σ	100	200	300	400	500
			increasing		
1.1					
(λ, h)	(0.03, 1.0343)	(0.02, 1.029)	(0.01, 1.0135)	(0.01, 1.016)	(0.01, 1.0183)
ARL_{min}	44.34	69.59	88.87	103.78	117.19
1.2					
(λ, h)	(0.06, 1.0977)	(0.03, 1.0547)	(0.02, 1.0382)	(0.02, 1.0784)	(0.03, 1.0860)
ARL_{min}	25.66	36.49	44.21	49.72	55.03
1.3					
(λ, h)	(0.07, 1.1231)	(0.06, 1.1445)	(0.04, 1.1015)	(0.04, 1.1150)	(0.04, 1.1260)
ARL_{min}	17.29	23.29	27.36	30.27	32.63
1.4					
(λ, h)	(0.09, 1.1758)	(0.06, 1.1445)	(0.05, 1.1375)	(0.05, 1.1546)	(0.05, 1.1685)
ARL_{min}	12.75	16.57	19.22	21.02	22.39
1.5					
(λ, h)	(0.13, 1.2891)	(0.10, 1.2852)	(0.09, 1.2954)	(0.08,1.2829)	(0.06, 1.2129)
ARL_{min}	10.01	12.64	14.35	15.57	16.61
1.6					
(λ, h)	(0.16, 1.3828)	(0.14, 1.4433)	(0.09, 1.2954)	(0.10,1.3759)	(0.08, 1.3061)
ARL_{min}	8.18	10.20	11.41	12.22	12.97
1.7					
(λ, h)	(0.18, 1.4453)	(0.17, 1.5633)	(0.12,1.4257)	(0.14, 1.5697)	(0.11, 1.4555)
ARL_{min}	6.89	8.42	9.34	10.08	10.57
2.0					
(λ, h)	(0.23, 1.6143)	(0.18, 1.6062)	(0.22,1.9009)	(0.21, 1.9358)	(0.16, 1.7199)
ARL_{min}	4.72	5.55	6.06	6.41	6.70
			decreasing		
0.9					
(λ, h)	(0.01, 1.0055)	(0.02, 1.0293)	(0.01, 1.0132)	(0.01, 1.0158)	(0.01, 1.0179)
ARL_{min}	49.51	76.78	97.27	113.81	127.68
0.8					
(λ, h)	(0.04, 1.0538)	(0.04, 1.0787)	(0.03, 1.0643)	(0.03, 1.0726)	(0.03, 1.0791)
ARL_{min}	29.22	40.87	48.30	53.94	58.54
0.7					
(λ, h)	(0.07, 1.1186)	(0.07, 1.1625)	(0.06, 1.1562)	(0.07,1.2065)	(0.06, 1.1845)
ARL_{min}	19.17	25.04	28.98	31.74	33.96
0.6					
(λ, h)	(0.14, 1.2961)	(0.11, 1.2828)	(0.12,1.3547)	(0.10, 1.3113)	(0.09, 1.2939)
ARL_{min}	13.50	16.93	19.12	20.67	21.91
0.5					
(λ, h)	(0.25, 1.5969)	(0.18, 1.5031)	(0.18, 1.5604)	(0.16, 1.5264)	(0.16, 1.5547)
ARL_{min}	9.79	12.11	13.47	14.43	15.21

Table 2
Optimal parameters of one-sided ELR charts based on sample size of n=5

	In-Control ARL				
σ	100	200	300	400	500
			increasing		
1.1					
(λ, h)	(0.05, 1.0161)	(0.04, 1.0172)	(0.03, 1.0140)	(0.03, 1.0159)	(0.03, 1.0175)
ARL_{min}	23.53	33.09	39.43	44.41	48.20
1.2					
(λ, h)	(0.10, 1.0437)	(0.08, 1.0445)	(0.08, 1.0522)	(0.06, 1.0398)	(0.06, 1.0430)
ARL_{min}	11.10	14.35	16.38	17.79	18.99
1.3					
(λ, h)	(0.16, 1.0820)	(0.15, 1.1008)	(0.15, 1.1158)	(0.09, 1.0668)	(0.13, 1.1132)
ARL_{min}	6.79	8.38	9.40	10.11	10.63
1.4					
(λ, h)	(0.29, 1.1805)	(0.21, 1.1545)	(0.21, 1.1758)	(0.15, 1.1262)	(0.18, 1.1685)
ARL_{min}	4.75	5.69	6.27	6.69	7.01
1.5					
(λ, h)	(0.33, 1.2133)	(0.27, 1.2125)	(0.26, 1.2301)	(0.19, 1.1691)	(0.21, 1.2039)
ARL_{min}	3.60	4.23	4.62	4.90	5.10
1.6					
(λ, h)	(0.42, 1.2925)	(0.30, 1.2429)	(0.32, 1.2976)	(0.24, 1.2258)	(0.31, 1.3285)
ARL_{min}	2.90	3.35	3.61	3.83	3.99
1.7					
(λ, h)	(0.43, 1.3035)	(0.34, 1.2844)	(0.33, 1.3101)	(0.34, 1.3484)	(0.33, 1.3555)
ARL_{min}	2.43	2.78	2.98	3.12	3.23
2.0					
(λ, h)	(0.53, 1.3992)	(0.50, 1.4653)	(0.45, 1.4578)	(0.45, 1.4945)	(0.40, 1.4515)
ARL_{min}	1.70	1.86	1.97	2.04	2.10
			decreasing		
0.9					
(λ, h)	(0.04, 1.0115)	(0.05, 1.0227)	(0.03, 1.0136)	(0.03, 1.0154)	(0.03, 1.0168)
ARL_{min}	25.40	35.10	41.21	46.05	49.96
0.8					
(λ, h)	(0.09, 1.0365)	(0.10, 1.0559)	(0.10, 1.0638)	(0.10, 1.0696)	(0.09, 1.0652)
ARL_{min}	11.78	14.61	16.50	17.87	18.9
0.7					
(λ, h)	(0.24, 1.1316)	(0.21, 1.1387)	(0.20, 1.1465)	(0.19, 1.1485)	(0.18, 1.1465)
ARL_{min}	6.89	8.08	8.96	9.56	10.01
0.6					
(λ, h)	(0.39, 1.2437)	(0.36, 1.2687)	(0.35, 1.2859)	(0.34, 1.2949)	(0.29, 1.2549)
ARL_{min}	4.32	5.13	5.61	5.97	6.22
0.5					
(λ, h)	(0.60, 1.4412)	(0.55, 1.4648)	(0.55, 1.5063)	(0.50, 1.4727)	(0.43, 1.4086)
ARL_{min}	3.00	3.52	3.83	4.04	4.22

Table 3
Optimal parameters of one-sided ELR charts based on sample size of n=10

	In-Control ARL				
σ	100	200	300	400	500
			increasing		
1.1					
(λ, h)	(0.07, 1.0133)	(0.07, 1.0186)	(0.04, 1.0105)	(0.04, 1.0117)	(0.04, 1.0127)
ARL_{min}	16.69	22.24	25.94	28.50	30.66
1.2					
(λ, h)	(0.13, 1.0313)	(0.13, 1.0418)	(0.12, 1.0435)	(0.11, 1.0428)	(0.11, 1.0457)
ARL_{min}	7.33	9.02	10.10	10.91	11.47
1.3					
(λ, h)	(0.25, 1.0750)	(0.23, 1.0869)	(0.20, 1.0826)	(0.19, 1.0841)	(0.19, 1.0895)
ARL_{min}	4.33	5.18	5.67	6.06	6.33
1.4					
(λ, h)	(0.33, 1.1078)	(0.33, 1.1377)	(0.26, 1.1148)	(0.26, 1.1244)	(0.25, 1.1254)
ARL_{min}	3.02	3.50	3.80	4.02	4.19
1.5					
(λ, h)	(0.42, 1.1476)	(0.41, 1.1816)	(0.34, 1.1611)	(0.37, 1.1933)	(0.35, 1.1906)
ARL_{min}	2.29	2.61	2.80	2.95	3.05
1.6					
(λ, h)	(0.62, 1.2484)	(0.55, 1.2660)	(0.51, 1.2701)	(0.47, 1.2621)	(0.39, 1.2185)
ARL_{min}	1.85	2.08	2.21	2.32	2.40
1.7					
(λ, h)	(0.62, 1.2484)	(0.61, 1.3046)	(0.54, 1.2906)	(0.47, 1.2621)	(0.50, 1.3001)
ARL_{min}	1.58	1.74	1.84	1.92	1.97
2.0					
(λ, h)	(0.69, 2883)	(0.66, 1.3379)	(0.63, 1.3563)	(0.50, 1.2836)	(0.61, 1.3884)
ARL_{min}	1.21	1.27	1.31	1.36	1.37
			decreasing		
0.9					
(λ, h)	(0.08, 1.0156)	(0.06, 1.0146)	(0.06, 1.0172)	(0.05, 1.0151)	(0.06, 1.0204)
ARL_{min}	17.35	22.87	26.57	29.14	31.31
0.8					
(λ, h)	(0.20, 1.0531)	(0.20, 1.0676)	(0.18, 1.0664)	(0.16, 1.0624)	(0.15, 1.0611)
ARL_{min}	7.25	8.89	9.89	10.62	11.14
0.7					
(λ, h)	(0.34, 1.1055)	(0.33, 1.1247)	(0.32, 1.1331)	(0.33,1.1477)	(0.31, 1.1437)
ARL_{min}	4.07	4.79	5.24	5.56	5.80
0.6					
(λ, h)	(0.59, 1.2227)	(0.54, 1.2375)	(0.52, 1.2606)	(0.50, 1.2497)	(0.50, 1.2619)
ARL_{min}	2.63	3.00	3.24	3.41	3.56
0.5					
(λ, h)	(0.84, 1.4062)	(0.82, 1.4625)	(0.83, 1.5145)	(0.61, 1.3278)	(0.62, 1.3505)
ARL_{min}	1.68	2.05	2.26	2.37	2.43

Table 4
zero-state ARL comparison for the upper-sided ELR, SJ and CH charts: increases in process standard deviation (n=5, IC ARL=200)

σ	$\lambda = 0.05$	0.1	0.2	0.3	0.5	0.7	0.9	1.0
				ELR				
	h^+=1.0236	1.0595	1.1454	1.2429	1.4653	1.7187	1.9966	2.141
1.0	200.21	199.92	200.71	199.87	198.99	199.82	201.02	201.25
1.1	33.54	35.29	39.89	44.21	50.96	55.68	59.16	60.22
1.2	14.63	14.38	15.29	16.68	19.54	22.12	24.18	24.90
1.3	9.10	8.52	8.49	8.92	10.07	11.34	12.45	12.80
1.4	6.52	5.95	5.72	5.80	6.30	6.91	7.54	7.76
1.5	5.07	4.57	4.29	4.25	4.44	4.77	5.11	5.27
1.6	4.17	3.73	3.44	3.37	3.43	3.59	3.80	3.90
1.7	3.53	3.14	2.88	2.81	2.78	2.87	3.00	3.06
1.8	3.07	2.74	2.50	2.41	2.38	2.41	2.49	2.53
1.9	2.72	2.43	2.22	2.13	2.08	2.10	2.14	2.17
2.0	2.44	2.19	2.00	1.93	1.87	1.87	1.90	1.92
				SJ				
	$L_W^+ = 1.568$	1.943	2.27	2.433	2.584	2.650	2.685	2.693
1.1	32.26	35.22	39.77	43.48	49.42	55.04	61.52	65.07
1.2	14.45	14.97	16.03	17.22	19.58	22.31	26.03	28.28
1.3	9.17	9.09	9.22	9.56	10.45	11.73	13.72	15.05
1.4	6.72	6.53	6.37	6.41	6.72	7.34	8.45	9.25
1.5	5.36	5.13	4.89	4.81	4.87	5.17	5.82	6.32
1.6	4.50	4.27	4.00	3.87	3.81	3.95	4.35	4.67
1.7	3.92	3.69	3.41	3.26	3.14	3.20	3.45	3.66
1.8	3.49	3.29	3.00	2.83	2.69	2.71	2.85	3.01
1.9	3.17	2.97	2.68	2.53	2.38	2.35	2.45	2.56
2.0	2.92	2.72	2.45	2.29	2.14	2.10	2.17	2.24
				CH				
	$L_Q^+ = 1.055$	1.303	1.513	1.598	1.657	1.667	1.652	1.634
1.1	43.01	44.19	46.52	48.51	52.50	57.11	62.38	65.07
1.2	18.09	18.23	18.81	19.48	21.12	23.46	26.56	28.28
1.3	10.75	10.57	10.55	10.69	11.27	12.36	14.03	15.05
1.4	7.62	7.36	7.14	7.08	7.21	7.72	8.65	9.25
1.5	5.97	5.69	5.41	5.26	5.19	5.42	5.95	6.32
1.6	4.96	4.69	4.39	4.21	4.05	4.13	4.44	4.67
1.7	4.28	4.03	3.73	3.53	3.33	3.34	3.51	3.66
1.8	3.80	3.56	3.27	3.06	2.85	2.80	2.92	3.01
1.9	3.44	3.22	2.92	2.73	2.50	2.44	2.50	2.56
2.0	3.17	2.96	2.67	2.47	2.25	2.18	2.20	2.24

Table 5
Steady-state ARL comparison for the upper-sided ELR, SJ and CH charts: increases in process standard deviation (n=5, IC ARL=200)

σ	$\lambda = 0.05$	0.1	0.2	0.3	0.5	0.7	0.9	1.0
				ELR				
	h^+=1.0236	1.0595	1.1454	1.2429	1.4653	1.7187	1.9966	2.141
1.0	200.85	200.34	200.68	199.53	200.72	198.18	201.43	198.21
1.1	29.88	32.91	38.65	43.14	50.15	54.50	59.10	60.22
1.2	12.54	12.95	14.50	16.22	19.38	22.07	24.15	24.90
1.3	7.64	7.53	7.96	8.50	9.87	11.23	12.38	12.80
1.4	5.45	5.24	5.27	5.48	6.10	6.82	7.52	7.76
1.5	4.28	4.02	3.94	4.01	4.30	4.71	5.13	5.27
1.6	3.50	3.29	3.17	3.17	3.32	3.55	3.80	3.90
1.7	2.97	2.78	2.66	2.64	2.70	2.83	2.98	3.06
1.8	2.60	2.42	2.30	2.27	2.30	2.38	2.48	2.53
1.9	2.32	2.16	2.05	2.01	2.02	2.07	2.14	2.17
2.0	2.10	1.97	1.86	1.83	1.82	1.84	1.90	1.91
				SJ				
	L_W^+=1.568	1.943	2.272	2.433	2.584	2.650	2.685	2.693
1.1	33.79	35.58	39.37	43.17	49.74	54.74	61.63	65.07
1.2	15.64	15.35	15.97	17.10	19.46	22.17	26.09	28.28
1.3	10.05	9.43	9.23	9.52	10.39	11.67	13.70	15.05
1.4	7.42	6.83	6.42	6.42	6.67	7.36	8.40	9.25
1.5	5.97	5.39	4.94	4.81	4.84	5.18	5.84	6.32
1.6	5.01	4.51	4.06	3.89	3.82	3.96	4.35	4.67
1.7	4.39	3.89	3.46	3.29	3.16	3.21	3.45	3.66
1.8	3.92	3.46	3.04	2.87	2.73	2.71	2.85	3.01
1.9	3.52	3.13	2.75	2.56	2.38	2.37	2.46	2.56
2.0	3.25	2.88	2.51	2.33	2.17	2.12	2.17	2.24
				CH				
	$L_Q^+ = 1.055$	1.303	1.513	1.598	1.657	1.667	1.652	1.634
1.1	40.89	42.51	45.17	47.31	51.94	57.14	62.37	65.07
1.2	16.65	17.14	18.01	18.78	20.54	23.23	26.48	28.28
1.3	9.71	9.67	9.88	10.23	10.88	12.18	14.07	15.05
1.4	6.82	6.66	6.58	6.62	6.91	7.55	8.63	9.25
1.5	5.29	5.10	4.96	4.87	4.97	5.32	5.85	6.32
1.6	4.39	4.20	3.99	3.88	3.84	4.00	4.41	4.67
1.7	3.78	3.60	3.38	3.24	3.15	3.24	3.47	3.66
1.8	3.34	3.18	2.95	2.81	2.68	2.72	2.89	3.01
1.9	3.02	2.87	2.63	2.50	2.36	2.37	2.47	2.56
2.0	2.80	2.62	2.40	2.27	2.13	2.12	2.18	2.24

Table 6
SDRL performance comparisons for dispersion: increase in process standard deviation (n=5, IC ARL=200)

	$\lambda = 0.1$			$\lambda = 0.3$		
σ	ELR	SJ	CH	ELR	SJ	CH
			Zero-state			
1.0	194.42	197.00	193.21	198.52	197.44	196.48
1.1	30.65	30.80	39.78	41.74	40.85	46.78
1.2	10.39	11.05	14.66	14.84	15.06	17.32
1.3	5.44	5.93	7.50	7.28	7.58	8.67
1.4	3.53	3.89	4.58	4.33	4.67	5.25
1.5	2.56	2.82	3.23	2.99	3.26	3.55
1.6	2.03	2.19	2.44	2.21	2.44	2.63
1.7	1.68	1.78	1.96	1.75	1.95	2.08
1.8	1.42	1.50	1.63	1.44	1.62	1.71
1.9	1.25	1.30	1.40	1.22	1.40	1.46
2.0	1.11	1.17	1.22	1.08	1.22	1.27
			Steady-state			
1.0	192.38	199.08	195.26	198.46	198.68	197.95
1.1	30.20	30.96	40.09	42.01	41.15	45.78
1.2	10.44	11.39	14.79	14.70	15.16	17.20
1.3	5.33	6.25	7.58	7.22	7.73	8.70
1.4	3.49	4.18	4.65	4.33	4.69	5.31
1.5	2.56	3.10	3.26	2.95	3.33	3.62
1.6	1.97	2.44	2.50	2.17	2.46	2.61
1.7	1.62	2.03	1.99	1.75	1.99	2.10
1.8	1.38	1.75	1.69	1.44	1.66	1.73
1.9	1.19	1.53	1.42	1.20	1.43	1.46
2.0	1.05	1.37	1.26	1.05	1.26	1.26

Table 7
Zero-state ARL comparison for the lower-sided ELR, SJ and CH charts: decreases in process standard deviation (n=5, IC ARL=200)

σ	$\lambda = 0.05$	0.1	0.2	0.3	0.5	0.7	0.9	1.0
				ELR				
	h^-=1.0227	1.0558	1.1316	1.2153	1.4082	1.6599	2.075	2.575
1.00	199.24	198.67	201.89	201.40	198.86	198.40	201.10	198.05
0.95	71.75	78.60	90.77	100.13	113.67	126.13	142.31	155.89
0.90	35.01	37.36	44.74	51.93	65.52	79.41	99.66	120.90
0.85	21.73	21.68	24.66	28.79	38.20	50.01	68.94	92.67
0.80	15.62	14.63	15.40	17.37	23.07	31.62	47.40	70.52
0.75	12.26	10.99	10.74	11.49	14.67	20.38	32.39	52.67
0.70	10.18	8.85	8.15	8.28	9.85	13.36	22.07	38.70
0.65	8.79	7.47	6.57	6.38	7.03	9.06	15.06	27.93
0.60	7.80	6.53	5.56	5.20	5.32	6.41	10.37	19.83
0.55	7.07	5.85	4.86	4.43	4.25	4.75	7.23	13.86
0.50	6.51	5.35	4.38	3.88	3.54	3.67	5.17	9.48
				SJ				
	L_W^- =2.21	2.84	3.521	3.95	4.525	4.855	5.038	5.05
0.95	96.45	108.98	124.64	134.86	150.09	156.58	163.03	163.10
0.90	51.60	61.36	77.63	89.45	109.58	122.41	131.00	132.45
0.85	30.78	36.68	48.45	59.28	78.84	92.90	104.23	106.92
0.80	20.01	23.37	30.76	38.92	55.65	69.50	81.28	84.62
0.75	14.02	15.65	20.05	25.60	38.83	51.20	62.06	66.24
0.70	10.25	11.06	13.51	16.99	26.57	37.00	47.57	51.42
0.65	7.82	8.18	9.47	11.59	18.16	26.43	35.41	38.80
0.60	6.16	6.29	6.96	8.16	12.38	18.48	25.88	29.19
0.55	4.96	4.96	5.27	5.93	8.58	12.80	18.54	21.24
0.50	4.09	4.03	4.12	4.49	6.02	8.79	13.05	15.30
				CH				
	L_Q^- =3.89	3.72	3.67	3.685	3.74	3.77	3.731	3.69
0.95	87.19	93.49	111.73	126.24	144.73	156.35	161.42	163.10
0.90	48.67	50.53	64.45	78.78	102.38	120.58	129.64	132.45
0.85	32.07	31.03	38.63	49.20	71.07	90.66	102.23	106.92
0.80	23.53	21.07	24.64	31.55	49.14	66.77	79.89	84.62
0.75	18.19	15.50	16.69	20.95	33.57	48.71	60.98	66.24
0.70	14.68	12.01	12.04	14.28	22.91	34.75	46.41	51.42
0.65	12.19	9.64	9.08	10.25	15.84	24.79	34.36	38.80
0.60	10.33	7.99	7.12	7.61	11.05	17.35	25.21	29.19
0.55	8.85	6.73	5.80	5.88	7.89	12.10	18.08	21.24
0.50	7.68	5.77	4.80	4.71	5.73	8.45	12.72	15.30

Table 8
Steady-state ARL comparison for the lower-sided ELR, SJ and CH charts: decreases in process standard deviation (n=5, IC ARL=200)

σ	$\lambda = 0.05$	0.1	0.2	0.3	0.5	0.7	0.9	1.0
				ELR				
	h^-=1.0227	1.0558	1.1316	1.2153	1.4081	1.6599	2.075	2.575
1.00	199.28	198.85	201.30	201.29	199.15	198.66	201.40	198.20
0.95	63.17	72.23	87.13	97.19	111.83	125.04	142.32	155.54
0.90	29.30	33.14	41.75	49.66	63.69	78.44	98.93	120.79
0.85	17.27	18.41	22.29	26.98	36.92	49.19	68.10	93.00
0.80	12.08	12.04	13.54	15.89	21.98	30.89	46.92	70.36
0.75	9.29	8.82	9.16	10.25	13.76	19.75	31.94	52.48
0.70	7.64	6.98	6.82	7.23	9.11	12.81	21.60	38.58
0.65	6.55	5.82	5.42	5.47	6.36	8.59	14.77	27.96
0.60	5.78	5.05	4.52	4.38	4.75	5.99	10.07	19.87
0.55	5.22	4.50	3.92	3.69	3.72	4.37	6.94	13.87
0.50	4.81	4.11	3.50	3.22	3.06	3.35	4.89	9.48
				SJ				
	L_W^- =2.21	2.84	3.521	3.95	4.525	4.855	5.038	5.05
0.95	98.41	108.81	124.47	135.33	149.38	157.39	162.62	163.84
0.90	53.96	61.89	78.14	89.43	109.70	121.46	131.65	132.68
0.85	32.66	37.06	48.49	59.16	78.78	92.38	103.86	107.35
0.80	21.46	23.53	30.64	38.76	55.74	69.26	81.93	84.92
0.75	15.15	15.93	20.00	25.45	38.64	51.32	62.47	66.71
0.70	11.21	11.37	13.63	17.01	26.63	37.21	47.27	51.39
0.65	8.58	8.44	9.54	11.66	18.15	26.54	35.34	39.13
0.60	6.81	6.49	6.97	8.15	12.37	18.43	25.82	28.95
0.55	5.53	5.16	5.31	5.95	8.53	12.79	18.48	21.33
0.50	4.56	4.22	4.18	4.49	6.01	8.83	13.05	15.26
				CH				
	L_Q^- =3.89	3.72	3.67	3.685	3.74	3.77	3.731	3.69
0.95	69.60	84.90	108.52	123.04	142.91	157.47	161.61	163.84
0.90	36.07	43.93	61.18	76.51	101.77	119.65	129.75	132.68
0.85	22.29	25.73	36.23	48.01	70.30	90.41	102.77	107.35
0.80	15.59	16.85	22.43	30.18	48.33	66.60	79.32	84.92
0.75	11.72	11.94	14.78	19.51	33.14	48.36	61.27	66.71
0.70	9.18	9.04	10.46	13.17	22.28	34.59	46.52	51.39
0.65	7.48	7.13	7.73	9.29	15.30	24.37	34.25	39.13
0.60	6.26	5.81	5.97	6.83	10.60	17.24	25.00	28.95
0.55	5.35	4.86	4.75	5.19	7.41	11.84	18.15	21.33
0.50	4.61	4.12	3.92	4.08	5.41	8.23	12.65	15.26

Table 9
SDRL performance comparisons for dispersion: decrease in process standard deviation (n=5, IC ARL=200)

	$\lambda = 0.1$			$\lambda = 0.3$		
σ	ELR	SJ	CH	ELR	SJ	CH
			Zero-state			
1.00	190.13	198.79	186.23	195.78	198.52	196.64
0.95	68.56	105.64	81.99	96.08	132.00	123.29
0.90	28.21	57.55	39.28	46.83	89.17	74.25
0.85	13.19	32.45	20.45	24.11	57.08	45.09
0.80	7.04	18.84	11.71	12.92	36.32	27.78
0.75	4.16	11.37	7.37	7.30	23.04	17.00
0.70	2.65	7.19	4.92	4.36	14.53	10.61
0.65	1.81	4.77	3.46	2.71	9.12	6.80
0.60	1.26	3.26	2.55	1.77	5.92	4.45
0.55	0.91	2.30	1.94	1.21	3.78	2.94
0.50	0.67	1.68	1.51	0.85	2.53	2.05
			Steady-state			
1.00	189.46	197.79	186.42	195.64	198.01	194.58
0.95	69.48	104.88	81.54	96.80	133.51	121.99
0.90	28.27	57.60	38.62	47.60	87.83	75.52
0.85	13.40	32.77	20.50	23.97	55.73	45.57
0.80	7.20	18.76	11.74	12.98	35.95	27.74
0.75	4.46	11.53	7.40	7.43	23.03	17.04
0.70	3.04	7.48	5.01	4.43	14.73	10.47
0.65	2.25	4.98	3.64	2.82	9.42	6.84
0.60	1.77	3.51	2.72	1.94	5.98	4.45
0.55	1.47	2.58	2.12	1.40	3.85	3.03
0.50	1.27	1.93	1.68	1.08	2.60	2.10

Table 10
Optimal OC ARL performance comparisons for dispersion: increase in process standard deviation (n=5, IC ARL=200)

	Zero-state							
		$\sigma_{opt} = 1.2$			$\sigma_{opt} = 1.4$			
σ	ELR	SJ	CH	CPC	ELR	SJ	CH	CPC
1.0	199.97	199.01	200.31	200.24	199.55	198.37	201.44	198.53
1.1	34.55	29.92	42.92	34.72	40.27	39.79	49.29	40.11
1.2	14.32	**13.96**	18.12	14.19	15.44	16.02	19.66	15.18
1.3	8.65	9.04	10.76	8.44	8.52	9.21	10.78	8.31
1.4	6.12	6.71	7.62	5.95	5.70	6.37	7.08	**5.56**
1.5	4.73	5.40	5.97	4.59	4.26	4.88	5.25	4.15
1.6	3.85	4.56	4.95	3.74	3.42	4.01	4.18	3.34
1.7	3.26	3.98	4.28	3.16	2.87	3.40	3.51	2.80
1.8	2.84	3.55	3.81	2.75	2.48	2.99	3.04	2.42
1.9	2.52	3.23	3.44	2.44	2.20	2.69	2.70	2.15
2.0	2.27	2.98	3.17	2.20	1.99	2.45	2.44	1.95
	Steady-state							
		$\sigma_{opt} = 1.2$			$\sigma_{opt} = 1.4$			
σ	ELR	SJ	CH	CPC	ELR	SJ	CH	CPC
1.1	31.84	34.42	40.82	32.56	39.09	39.07	48.12	39.12
1.2	**12.76**	16.61	16.71	12.99	14.67	15.87	19.01	14.71
1.3	7.56	10.87	9.74	7.61	7.97	9.21	10.22	7.98
1.4	5.30	8.17	6.82	5.35	**5.30**	6.41	6.68	5.30
1.5	4.10	6.59	5.30	4.13	3.94	4.95	4.90	3.95
1.6	3.34	5.58	4.39	3.38	3.14	4.06	3.89	3.18
1.7	2.83	4.86	3.79	2.86	2.65	3.48	3.23	2.67
1.8	2.48	4.33	3.36	2.49	2.29	3.06	2.78	2.32
1.9	2.21	3.94	3.06	2.23	2.04	2.74	2.48	2.06
2.0	2.00	3.62	2.81	2.02	1.86	2.53	2.25	1.87

Table 11
Optimal OC ARL performance comparisons for dispersion: decrease in process standard deviation (n=5, IC ARL=200)

	Zero-state							
	$\sigma_{opt} = 0.8$				$\sigma_{opt} = 0.6$			
σ	ELR	SJ	CH	CPC	ELR	SJ	CH	CPC
1.0	199.27	200.68	198.99	199.49	200.12	200.68	199.96	199.44
0.9	37.47	49.24	50.64	38.37	55.80	49.24	64.45	59.59
0.8	14.66	19.36	21.06	14.17	18.79	19.36	24.64	19.57
0.7	8.86	10.07	12.00	8.25	8.56	10.07	12.04	8.30
0.6	6.53	6.11	7.99	5.97	5.14	6.11	7.14	4.73
0.5	5.36	4.09	5.77	4.82	3.73	4.09	4.80	3.35
0.4	4.69	2.94	4.36	4.16	3.12	2.94	3.47	2.67
0.3	4.08	2.22	3.37	4.00	2.91	2.22	2.63	2.17
0.2	4.00	1.76	2.62	3.98	2.41	1.76	2.02	2.00
	Steady-state							
	$\sigma_{opt} = 0.8$				$\sigma_{opt} = 0.6$			
σ	ELR	SJ	CH	CPC	ELR	SJ	CH	CPC
1.0	199.81	200.14	199.57	199.72	200.32	200.71	199.94	200.18
0.9	33.28	52.38	50.51	35.05	53.58	52.38	64.69	58.11
0.8	12.02	21.35	21.06	12.26	17.49	21.35	24.69	18.73
0.7	7.02	11.42	11.95	7.01	7.62	11.42	12.03	7.78
0.6	5.06	7.00	7.99	5.01	4.32	7.00	7.13	4.36
0.5	4.11	4.71	5.77	4.06	3.13	4.71	4.80	3.06
0.4	3.59	3.39	4.36	3.52	2.55	3.39	3.47	2.46
0.3	3.24	2.55	3.37	3.29	2.26	2.55	2.62	2.04
0.2	3.09	1.95	2.62	3.16	1.99	1.95	2.02	1.90

Table 12
Two-sided zero-state OC ARL comparison(n=5, IC ARL=200)

	$\lambda = 0.05$				$\lambda = 0.1$			
σ	ELR	SJ	CH	CPC_1	ELR	SJ	CH	CPC_2
0.5	6.59	5.36	5.34	6.50	5.45	4.95	4.78	4.85
0.6	7.91	8.13	7.41	7.77	6.68	7.89	6.94	5.99
0.7	10.35	13.90	11.15	10.14	9.14	14.59	11.24	8.38
0.8	16.03	28.61	19.88	15.71	15.69	33.72	22.77	15.04
0.9	39.17	84.47	52.98	38.04	46.36	103.40	69.98	48.49
1.0	200.92	200.46	200.02	201.89	200.54	199.43	201.59	199.36
1.1	38.21	45.05	59.73	38.33	41.24	48.89	63.35	43.86
1.2	15.72	19.33	21.74	15.87	15.44	19.03	22.68	15.94
1.3	9.56	11.95	11.95	9.78	8.96	11.19	12.04	9.12
1.4	6.83	8.73	8.14	6.99	6.24	7.90	7.95	6.33
1.5	5.29	6.92	6.24	5.43	4.76	6.12	6.00	4.84
1.6	4.30	5.75	5.09	4.42	3.85	5.07	4.87	3.91
1.7	3.65	4.98	4.37	3.74	3.26	4.35	4.13	3.30
1.8	3.17	4.44	3.86	3.25	2.81	3.84	3.61	2.85
1.9	2.80	4.01	3.47	2.87	2.50	3.47	3.24	2.54
2.0	2.52	3.68	3.18	2.59	2.26	3.18	2.96	2.28
	$\lambda = 0.2$				$\lambda = 0.3$			
σ	ELR	SJ	CH	CPC_3	ELR	SJ	CH	CPC_4
0.5	4.52	5.05	4.64	3.99	4.13	5.66	5.06	3.52
0.6	5.83	8.94	7.45	5.21	5.68	11.14	9.10	5.04
0.7	8.85	19.19	14.16	8.12	9.71	25.90	19.70	9.28
0.8	18.31	49.25	34.79	17.94	23.49	65.93	50.66	25.00
0.9	66.62	137.99	107.46	68.42	90.12	164.41	138.61	92.69
1.0	199.79	200.12	199.65	200.01	200.81	201.47	199.88	200.18
1.1	47.24	56.94	67.24	50.28	52.61	64.58	70.86	56.02
1.2	16.71	21.13	24.26	16.99	18.38	23.48	25.79	18.59
1.3	8.97	11.40	12.48	9.14	9.44	12.06	12.98	9.53
1.4	5.95	7.58	7.97	6.14	6.05	7.78	8.12	6.17
1.5	4.44	5.74	5.79	4.60	4.41	5.68	5.79	4.56
1.6	3.53	4.61	4.58	3.69	3.46	4.47	4.48	3.62
1.7	2.96	3.90	3.85	3.10	2.86	3.74	3.69	3.01
1.8	2.56	3.41	3.33	2.68	2.46	3.24	3.19	2.59
1.9	2.27	3.07	2.96	2.37	2.17	2.87	2.80	2.29
2.0	2.04	2.78	2.68	2.13	1.96	2.60	2.50	2.07